

Stimulation Calculation of Desulfurization Mechanisms Dominated by Free Radicals Reactions During Pyrolysis of Thiophenes Under Water Vapor Atmosphere

Ya Cheng

Inner Mongolia University

Jianping Chen

Inner Mongolia Medical University

Huiqing Guo

Inner Mongolia Medical University

Yanqiu Lei

Inner Mongolia University

Fenrong Liu (✉ fenrongl@163.com)

Inner Mongolia University

Research Article

Keywords: Desulfurization mechanism, Steam atmosphere, Thiophene compounds, Pyrolysis, Free radicals

Posted Date: August 20th, 2021

DOI: <https://doi.org/10.21203/rs.3.rs-825741/v1>

License:   This work is licensed under a Creative Commons Attribution 4.0 International License.

[Read Full License](#)

1 **Stimulation calculation of desulfurization mechanisms dominated by**
2 **free radicals reactions during pyrolysis of thiophenes under water**
3 **vapor atmosphere**

4 **Ya Cheng^a, Jianping Chen^b, Huiqing Guo^{b*}, Yanqiu Lei^a and Fenrong Liu^{a*}**

5 ^a College of Chemistry and Chemical Engineering, Inner Mongolia University,
6 Hohhot 010021, China

7 ^b School of Pharmaceutical Science, Inner Mongolia Medical University, Hohhot
8 010110, China

9 *Corresponding author. Phone/Fax: +86-471-4992981.

10 E-mail: fenrongl@163.com, gvohq@immu.edu.cn

11 Ya Cheng and Jianping Chen contributed equally to this work.

12 **Abstract:** The desulfurization mechanisms of thiophene and 2-methyl thiophene were
13 investigated by the density functional theory (DFT) during pyrolysis under water
14 vapor atmosphere. All possible reaction pathways of these desulfurization mechanisms
15 were explored at M06-2X/6-311g (d) level. The Multwfn3.0 and VMD1.9.2 programs
16 were used to analyze weak interactions between thiophene compounds and H₂O
17 molecule. It can be seen that hydrogen bonds can be formed in the reactions of
18 thiophene sulfurs and H₂O. Since H₂O molecule can decompose at higher
19 temperature and generate free radicals, such as •H and •OH, , the desulfurization
20 mechanisms of thiophene and 2-methyl thiophene with free radicals need to be further
21 considered. The reaction energy barriers (ΔG^\ddagger) and reaction energies (ΔG_p) of
22 thiophene and 2-methyl thiophene with H₂O molecule (g) or free radicals (•H and •OH)

23 have been stimulated and calculated in detail. Based on the transition state theory
24 (TST), the rate constants corresponding to these elementary reactions are also
25 calculated, meanwhile the speed and spontaneity of every reaction can be obtained
26 from the aspect of kinetics. Theoretically, it is found that H₂O (g) directly attacking
27 C-S bonds of thiophene and 2-methyl thiophene cannot easily generate COS and H₂S
28 even at 1200 K in terms of thermodynamics and kinetics. If the desulfurization
29 mechanisms of thiophenes are investigated by free radicals mechanisms under steam
30 atmosphere, their initial energy barriers needing to be overcome significantly reduce.
31 Therefore, desulfurization mechanisms of thiophenes and H₂O (g) are the most
32 possibly dominated by radical reactions at higher temperatures and H₂S is mainly
33 generated.

34 **Keywords:** Desulfurization mechanism; Steam atmosphere; Thiophene compounds;
35 Pyrolysis; Free radicals

36 **1. Introduction**

37 China consumes the most coal worldwide. The sulfur and nitrogen heteroatoms in
38 coal would be converted to sulfur-containing gases (COS, H₂S, SO_x) and nitrogen
39 oxides (NO_x)¹. Thus, massive utilization of coal can cause various environmental
40 issues, such as air pollution and acid rain. Therefore, Sulfur removal before the toxic
41 sulfur compounds are released into the environment is also an important subject ².

42 Hydrous pyrolysis was used to simulate desulfurization reaction and the obtained
43 data suggest that water acts like a reactant³. But, the detailed desulfurization
44 mechanism under steam atmosphere remains unclear⁴. Aliphatic sulfur compounds,

45 such as thiols and sulfides, have been found to react during the experiment of
46 hydrothermal simulation in 473-603K. Liu et al.³ found that the increasing of the feed
47 ratio of water to thiophene facilitates desulfurization and more gases were generated.
48 Abraham and Klein⁵ investigated the reaction of benzylphenyl sulfide (BPS) in
49 subcritical water and observed benzaldehyde as the major product, indicating that water
50 was involved as a reactant. Thus, water vapor has been used as an atmosphere to
51 investigate desulfurization behavior during coal pyrolysis. As large quantities of H₂
52 and expensive catalysts were required during the conventional hydro desulfurization
53 process, water vapor pyrolysis can be considered as a potential alternative
54 desulfurization method to reduce sulfur content in high sulfur coals. Water vapor
55 attacks C-S bond of thiophene which results in the breakage of the C-S bond, and H₂S,
56 CO, CO₂, H₂, light hydrocarbons and other gases are produced during the hydrothermal
57 cracking of thiophene^{6,7,8}. Under steam atmosphere, H and OH free radicals are easily
58 formed at high temperature. Wang et al.⁹ has focused on the effect of steam on the
59 transformation of sulfur during coal pyrolysis at the range of temperatures from 573 to
60 1073K. The removal of organic sulfur was found to increase, because the addition of
61 steam above 773K promoted the decomposition of thiophenic sulfur. In addition,
62 steam can generate more •H radicals, promoting the formation of H₂S⁹.

63 There have been several experimental studies about the desulfurization behaviors
64^{10,11,12}, but few have focused on the detailed desulfurization mechanism at the micro
65 level. Quantum chemistry can be used to calculate the thermochemical properties of
66 coal, the interaction between coal surface and gas, the desulfurization mechanism of

67 sulfur-containing model compounds and their pyrolysis reactions^{13,14,15,16}. It can also
68 help explaining some unclear phenomena in the experiments at a theoretical level. Yuko
69 Kida et al.⁹ used quantum chemistry to calculate the radical reactions of C-S bond
70 cleavage in hexyl sulfide and the addition of water to the C=S bond to form a geminal
71 mercaptoalcohol in the supercritical water (SCW) experiment. The mercaptoalcohol
72 then decomposes into an aldehyde and H₂S either directly or via a water-catalyzed
73 6-membered ring transition state. So their results showed that H₂O is a reactant and can
74 participate in the decomposition reaction of hexyl sulfide. Other theoretical studies
75 have also shown H₂O can reduce the energy barrier of gas phase single molecular
76 reactions in several systems^{17,18,19}. In recent years, interactions between water
77 molecules and coal models have been extensively studied^{20,21,22}. Water molecules tend
78 to accumulate around oxygen-containing functional groups of coal models and
79 hydrogen bonds play a leading role in the interaction according to the Reduced Density
80 Gradient (RDG) analysis²³.

81 Because of the variably complicated three-dimensional macromolecular structure of
82 coal, it is difficult to build coal itself via modeling tools. The homolytic energy of
83 monocyclic aromatic compounds often can be used to predict the homolytic energy of
84 polycyclic aromatic compounds with similar structures. Thus, in this study, thiophene
85 and 2-methyl thiophene were selected to represent the difficult-to-remove coal-based
86 sulfur species and to investigate their detailed desulfurization mechanisms during
87 pyrolysis under steam atmosphere. All possible desulfurization pathways of these
88 thiophenes were calculated and analyzed from the perspective of thermodynamics and

89 kinetics. Therefore, the detailed desulfurization mechanisms of these thiophenes can
90 be obtained under steam atmosphere. This can provide some theoretical basis for coal
91 desulfurization during coal utilization under steam atmosphere.

92 **2. Calculation methods**

93 **2.1 Geometry optimization and energy evaluation**

94 All quantum chemistry calculations were carried out using the Gaussian 09 software
95 package²⁴. Geometry optimization of various reactants, products, intermediate (IMn)
96 and transition states (TSn) were calculated by using the mixed element exchange
97 correlation function M06-2X^{25,26} with the standard base group 6-311g(d) in density fun
98 ctional theory (DFT), and the thermodynamic correction was calculated at the same
99 theoretical level. M06-2X with Grimme's DFT-D3 dispersion correction using the
100 Becke-Johnson damping function is highly suitable and reliable for noncovalent
101 interaction calculations^{27,28}. Moreover, for each transition state calculations of intrinsic
102 reaction coordinate (IRC) and vibration analysis, using a same basis set for
103 computational rationality (M06-2X/6-311g(d)), were used to confirm the connections
104 between the reactants and products correspondingly. The transition state has only one
105 imaginary frequency^{18,29,30}, and all other species have real frequency.
106 M06-2X/def2tzvp was used to calculate the single point energy which was added to the
107 thermodynamic correction amount to obtain the energy barrier (ΔG^\ddagger) of each step
108 reaction. Reaction energy (ΔG_p) was used to judge whether the reaction is spontaneous.
109 All relative energy barrier (ΔG^\ddagger) and reaction energy (ΔG_p) were obtained via
110 equations (1) and (2)

111
$$\Delta G^\ddagger = G^{\text{TS}} - G^{\text{IM}} \quad (1)$$

112
$$\Delta G_{\text{P}} = G_{\text{P}} - G_{\text{R}} \quad (2)$$

113 where G_{P} , G_{R} , G_{TS} , G_{IM} are the Gibbs free energy of the corresponding product (P),
114 reactant (R), transition state (TSn) and intermediate (IMn) of a pathway, respectively.

115 **2.2 The Reduced Density Gradient (RDG) Analysis**

116 The Reduced Density Gradient (RDG)³¹ method was used to define a real space
117 function, and the points in space and the sign $[\lambda_2(\mathbf{r})]\rho(\mathbf{r})$ function were used as
118 coordinates to make a RDG diagram by the wave function program Multiwfn3.4.1³²
119 and the visualization program VMD1.9.2³³. The RDG diagram can manifest weak
120 interaction areas between molecules and inter molecules. The smaller value $[\lambda_2(\mathbf{r})]\rho(\mathbf{r})$
121 of the scatter ($\rho > 0$, $\lambda_2 < 0$) indicates that the interaction is of stronger attractive
122 (H-bonds). The higher sign $[\lambda_2(\mathbf{r})]\rho(\mathbf{r})$ of the scatter ($\rho > 0$, $\lambda_2 > 0$) indicates that the
123 interaction is a repulsive force. If the sign $[\lambda_2(\mathbf{r})]\rho(\mathbf{r})$ of the scatter is close to zero ($\rho \approx 0$,
124 $\lambda_2 \approx 0$), this interaction is Van der Waals (vdW) forces. The complex structures of
125 thiophene sulfurs and H₂O have been optimized at the M06-2X/6-311g (d) level and
126 used for RDG analysis. The RDG function equation is

127
$$\text{RDG}(\mathbf{r}) = \frac{1}{2(3\pi^2)^{1/2}} \frac{|\nabla\rho(\mathbf{r})|}{\rho(\mathbf{r})^{4/3}}$$

128 where $\rho(\mathbf{r})$ is the electron density varying with \mathbf{r} .

129 **2.3 Reaction rate constant calculation**

130 The rate constants of reactions of thiophene sulfurs and water vapor can be
131 obtained according to the following equation³⁴,

132
$$k(T) = \frac{K_B T}{h} \left(\frac{Q_{TS}}{Q_R} \right) \exp\left(-\frac{E_a}{K_B T}\right)$$

133 where K_B , T , and E_a are the Boltzmann constant, reaction temperature (298 K), and
 134 activation energy, respectively. Q_{TS} and Q_R are the partition functions per unit volume
 135 for a TS and a reactant, respectively.

136 **3 Results and discussion**

137 In this study, thiophene ()₁, 2-methyl thiophene ()₂ were selected to
 138 investigate their desulfurization mechanisms during pyrolysis under steam atmosphere.
 139 During pyrolysis, water vapor maybe directly attack C-S bonds, or water vapor
 140 dissociates and forms free radicals ($\bullet\text{H}$ and $\bullet\text{OH}$). Free radicals then attack C-S bonds
 141 or / and other carbon sites, and H_2S , CO , H_2 , light hydrocarbons and other gases could
 142 be generated [3]. Therefore, we aim to investigate the addition reactions of H_2O and
 143 C-S bonds of thiophene sulfurs and radical reactions of free radicals and thiophenes
 144 and obtained the most possible desulfurization mechanisms of thiophenes and H_2O .

145 **3.1 RDG analysis of thiophenes and H_2O**

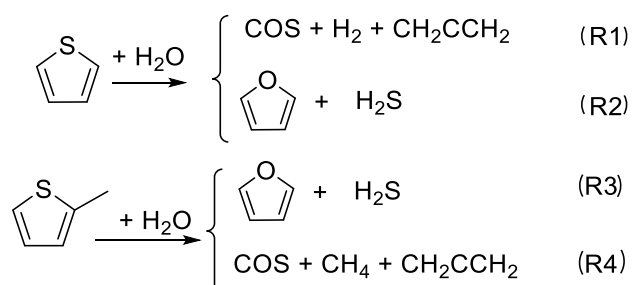
146 Fig. 1 shows the RDG diagrams of complexes (i.e., A and B) formed by two typical
 147 thiophenes with H_2O (g). The RDG diagram of complex A is of thiophene and H_2O
 148 (g). The large green or brown-green isosurface indicates that the weak vdW
 149 interaction in complex A is quite obvious, corresponding to the spikes at the scattered
 150 value range from -0.01 a.u. to 0.01 a.u. The fusiform red isosurface in the thiophene
 151 ring indicates that the ring itself has spatial repulsion (see the spike at the range from
 152 0.035 a.u. to 0.040 a.u.).

153 The RDG diagram of complex B is of H_2O and 2-methyl thiophene. For complex B,

154 S atom of 2-methyl thiophene and H atom of H₂O can form distinct H-bond at the
 155 scattered value of -0.040 a.u. to -0.035 a.u., and there also is a large spatial repulsive
 156 force between O in H₂O and C5 on 2-methylthiophene, corresponding to the spikes at
 157 the value ranging from 0.020 a.u. to 0.030 a.u..

158 3.2 Desulfurization mechanisms of thiophenes with H₂O (g) addition reactions

159 Recently, for the better desulfurization effect and higher tar yield of coal, the
 160 supplement of hydrogen source is the most effective method. Water vapor used for
 161 pyrolysis desulfurization is a relative cheap and easily available hydrogen source.
 162 Thus, in order to investigate the effect of water molecules on desulfurization
 163 mechanisms, the reaction mechanisms of H₂O (g) or free radicals (•H and •OH) with
 164 thiophenes were calculated and investigated. The most possible pathways of
 165 thiophenes and H₂O (g) are considered as follows:



166

167 3.2.1 Desulfurization mechanisms of thiophenes with H₂O

168 Fig. 2 illustrates the energy diagrams of thiophene and H₂O forming COS (R1) and
 169 H₂S (R2) at 1200 K. For R1, H₂O firstly attacks C2 site in thiophene and forms
 170 intermediate IM1 by overcoming the energy barrier (145.6 kcal/mol) of TS1,
 171 meanwhile one molecule of H₂ is removed. Then, IM2 is formed through TS2 after
 172 overcoming a 64.9 kcal/mol energy barrier. Subsequently, H migration occurs from
 173 C4 to C5 in IM2 and then IM3 is generated. Lastly, C-S, C-C bonds of IM3 are

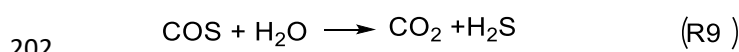
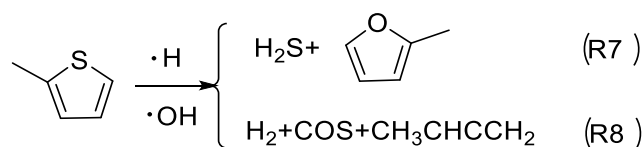
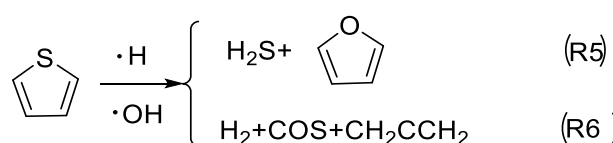
174 broken, and COS, H₂ and CH₂CCH₂ are generated. In R2, the H···OH bond in H₂O is
175 extended from the original 0.97Å to 1.02Å by the transition state TS1 and is added to
176 the C-S bond of thiophene to form intermediate IM1. Then, H migration in IM1
177 occurs after overcoming a 46.6 kcal/mol barrier and IM2 is formed. Lastly, IM2
178 undergoes the closed-loop reaction and forms furan, meanwhile one molecular H₂S is
179 removed. Thermodynamically and dynamically, H₂O (g) attacking C-S bonds of
180 thiophene cannot easily generate COS and H₂S at 1200 K, as the ΔG_p of R1 and R2
181 are 2.8 kcal/mol and 11.8 kcal/mol, respectively.

182 Fig. 3 is the energy diagram of 2-methyl thiophene and H₂O (g) forming H₂S (R3)
183 and COS (R4) at 1200 K. In R3 and R4, the formation of their IM1s needs to
184 overcome the higher initial reaction energy barriers of 116.3 kcal/mol and 147.3
185 kcal/mol, respectively. For R3, IM1 undergoes an closed-loop reaction and
186 intramolecular hydrogen migration and C-S bonds cleavage to form 2-methylfuran
187 and H₂S. The ΔG_p of R3 is 3.9 kcal/mol. IM1 in R4 undergoes two-step H migration
188 and IM3 is generated. Then, C-S, C-C bonds of IM3 are broken and COS, CH₄ and
189 CH₂CCH₂ are generated. R3 are thermodynamically non-spontaneous. Although
190 reaction R4 ($\Delta G_p = -13.4$ kcal/mol) is thermodynamically spontaneous, it needs to
191 overcome a very high energy barrier. Thus, it is also not easy to generate H₂S and
192 COS at 1200 K for H₂O with thiophene and 2-methyl thiophene through R3 and R4.

193 **3.2.2 Desulfurization mechanisms of thiophenes with free radicals (•H and •OH)**

194 Free radicals play a crucial role in coal pyrolysis process³⁵. H and OH free radicals
195 generation, stabilization and condensation easily occur during water vapor treatment

196 and coal pyrolysis progress^{36,37}. The removal of organic sulfur was found to increase,
 197 because the addition of steam results in generating more H free radicals promoting the
 198 generation of H₂S⁹. Based on these results, desulfurization reactions of thiophenes
 199 with free radicals ($\cdot\text{H}$ and $\cdot\text{OH}$) were proposed and investigated under steam
 200 atmosphere. The possible desulfurization pathways of thiophene, 2-methyl thiophene
 201 and free radicals are considered as follows:



202
 203 Fig. 4 shows energy diagrams of thiophene and $\cdot\text{H}$ and $\cdot\text{OH}$ forming H₂S (R5) and
 204 COS (R6) at 1200 K. H and OH radicals are mainly derived from the decomposition
 205 of water vapor [36] and coal [37]. For R5, firstly, H radical is adsorbed on the C2 site
 206 of thiophene, and the unstable cyclic thiophene radical (R) is formed after overcoming
 207 a 1.9 kcal/mol energy barrier. Then, OH radical combines with the C5 site in R with
 208 only a 41.7 kcal/mol barrier and IM1 is generated. Subsequently, IM3 is formed by
 209 two steps of hydrogen transferring. Lastly, IM3 transforms into H₂S and furan through
 210 C-S bond breakage with a low energy barrier of 20.2 kcal/mol. For R6, the energy
 211 barrier of transition state from IM1 to IM2 (80.3 kcal/mol) is very high. Then, IM2
 212 undergoes H migrations from C3 site to C4 site and IM3 is formed through
 213 overcoming an energy barrier of 72.8 kcal/mol. Lastly, COS, H₂ and CH₂CCH₂ are

214 formed by C-C and C-S bonds cleavage of IM3. As of its high energy barrier, it is also
215 impossible for R6 to occur. Thus, H₂S is the main product during thiophene
216 desulfurization under steam atmosphere. Compared with the reactions of thiophene
217 with H₂O, its desulfurization mechanism should be dominated by radical reactions at
218 high temperatures in water vapor atmosphere. These results can further prove that the
219 hydrogen radicals significantly reduce the energy barrier of thiophene desulfurization
220 reaction. The reason is that • H can damage the aromaticity of thiophene according to
221 the anisotropy of the induced current density (ACID) analysis [15] to form unstable
222 complex cyclic thiophene radical (R).

223 Fig. 5 lists the energy diagrams of 2-methyl thiophene with • H and • OH forming
224 H₂S (R7) and COS (R8) at 1200 K. For R7 and R8, dynamically, • H firstly combines
225 with C2 or C5 sites of 2-methyl thiophene to form 2-methyl thiophene radical (R) by
226 overcoming only a 8.0 or 3.1 kcal/mol energy barrier, respectively. And this energy
227 barrier is lower than the total reactants energy of 2-methyl thiophene and • H. OH
228 radical then attacks C5 or C2 sites to form a complex IM1 after overcoming the
229 energy barrier of 45.0 or 47.6 kcal/mol, respectively. IM1 in R7 undergoes two-step H
230 migration and IM3 is generated. Then, a closed-loop reaction occurs and a molecule
231 of H₂S is removed through TS4 to form H₂S and 2-methyl furan after overcoming a
232 low energy barrier of 23.8 kcal/mol. For R8, IM1 undergoes similar reaction steps as
233 R6 and generates COS, H₂ and CH₃CHCCH₂. These calculated results show that
234 thiophenes reacting with • H and • OH can generate COS, H₂S and small molecular
235 hydrocarbons. But, COS is unstable compared with H₂S³⁸, as it can be converted to

236 H₂S (R9) in steam atmosphere in the reactor³⁹. Consistent with some previous
237 experimental conclusions, sulfur-containing gases are mainly H₂S during pyrolysis of
238 thiophenes in water vapor system^{3,9}. Therefore, at higher temperatures, thiophenes
239 desulfurization mechanisms are most likely dominated by radical reactions under steam
240 atmosphere.

241 **3.3 Rate constant analysis**

242 In order to investigate the effect of reaction temperatures and H₂O (g) / radicals
243 on desulfurization mechanisms of thiophene and 2-methyl thiophene, the reaction rate
244 constant of each path was calculated between 700K - 1200K by transition state theory³⁹
245 (TST) and listed in Table 1. R1, R2 and R3 are thermodynamically unfeasible even at
246 1200 K, so their reaction rate constants are not considered. As shown in Table 1, R4 is
247 the reaction path of thiophene sulfur and H₂O (g) for forming COS. R5 and R7 are the
248 paths of thiophene and 2-methyl thiophene with free radicals for generating H₂S,
249 respectively. R6 and R8 are the paths of thiophene and 2-methyl thiophene with free
250 radicals to generate COS, respectively. All these rate constants increase with the
251 increasing of the reaction temperatures from 700K and 1200 K. The rate constants rank
252 of generating H₂S and COS is: $k[R7] > k[R5] > k[R6] > k[R8] > k[R4]$ at 1200K. For R5
253 (R7), the rate constant for generating H₂S is higher about 10^3 times than that of COS
254 (R6 and R8) at 1200K. This further indicates that the sulfur-containing gases
255 generated by the reaction of thiophenes and free radicals are mainly H₂S. The rate
256 constants of COS formation in R6 and R8 are about 3×10^{10} times higher than that of

257 R4 at 1200 K. This further proves that $\cdot\text{OH}/\cdot\text{H}$ participation is more beneficial for COS
258 formation than H_2O (g) during thiophenes desulfurization.

259 **4. Conclusions**

260 The desulfurization mechanisms of thiophene and 2-methyl thiophene under steam
261 atmosphere have been investigated in detail. The following conclusions can be drawn:

262 H_2O attacking C-S bond of thiophene and 2-methyl thiophene cannot kinetically and
263 thermodynamically form H_2S and COS even at 1200 K, as their higher reaction energy
264 barriers need to be overcome. The reaction energies of these thiophenes with free
265 radicals can reduce significantly compared with H_2O molecule.

266 At higher temperature, thiophenes and free radicals can kinetically and
267 thermodynamically react and form H_2S and COS. And H_2S is the main
268 sulfur-containing gases, its rate constant further proves that rate of generating H_2S is
269 faster than COS. Therefore, the most possible mechanisms for the removal of
270 thiophenes are dominated by free radical reaction mechanisms in water vapor
271 atmosphere at high temperatures. This can provide some theoretical basis for the
272 desulfurization mechanisms of sulfurs in coals during pyrolysis.

273 **Acknowledgements**

274 This study was financially supported by the Projects of Natural Science Foundation
275 of China (No. 21865018) and the Project Natural Science Foundation of Inner
276 Mongolia (No. 2018MS02005). We also thank Dr. Sobereva for his enlightening
277 advice on DFT calculations.

278 **References**

- 279 1. Liu, J. et al. Theoretical study of the effect of hydrogen radicals on the formation
280 of HCN from pyrrole pyrolysis. *J. Energy Inst.* 92,1468-1475(2019).
- 281 2. Liu, F. et al. Py-MS study of sulfur behavior during pyrolysis of high-sulfur coals
282 under different atmospheres. *Fuel Processing Technology*;91,1486-1490 (2010).
- 283 3. Liu, Y. et al. Equilibrium calculation of thiophene hydrolysis and reaction
284 mechanism analysis. *Journal of Chemical Industry and Engineering* 56,6-10
285 (2005). (in Chinese)
- 286 4. Vogelaar, B. M. et al. Applicability of supercritical water as a reaction medium
287 for desulfurisation and demetallisation of gasoil. *Fuel Process. Technol.*
288 61,265-277(1999).
- 289 5. Abraham, M. A. et al. Reactions of benzyl phenyl sulfide neat and in dense polar
290 solvents. *Fuel Sci. Technol. Int.* 6,633-662(1988).
- 291 6. Clark, P. D. et al. Chemistry of organosulphur compound types occurring in
292 heavy oil sands 1. High temperature hydrolysis and thermolysis of
293 tetrahydrothiophene in relation to steam stimulation processes. *Fuel.*
294 62,959-962(1983).
- 295 7. Clark, P. D. et al. Some chemistry of organosulphur compound types occurring in
296 heavy oil sands 2. Influence of pH on the high temperature hydrolysis of
297 tetrahydrothiophene and thiophene. *Fuel.* 63,125-128(1984).
- 298 8. Clark, P. D. et al. Chemistry of organosulphur compound types occurring in
299 heavy oil sands 3. Reaction of thiophene and tetrahydrothiophene with vanadyl
300 and nickel salts. *Fuel.* 63,1649-1654(1984).

- 301 9. Wang, M. et al. Effect of steam on the transformation of sulfur during
302 demineralized coal pyrolysis. *J. Anal. Appl. Pyrolysis*. 140,161-169(2019).
- 303 10. Yang, N. et al. Effects of atmospheres on sulfur release and its transformation
304 behavior during coal thermolysis. *Fuel*. 215,446-453(2018;).
- 305 11. Shao, D. et al. Behavior of sulfur during coal pyrolysis. *J. Anal. Appl. Pyrolysis*.
306 30,91-100(1994).
- 307 12. Yan J. et al. SH Radical: The key intermediate in sulfur transformation during
308 thermal processing of coal. *Environ. Sci. Technol*. 2005;39,5043-5051.
- 309 13. Gao, Z, et al. Adsorption mechanism of lignite and water molecules. *Journal of*
310 *China Coal Society*. 42,505-511 (2017). (in Chinese)
- 311 14. Nguyen, T. L. et al. Theoretical study of reaction of ketene with water in the gas
312 phase: formation of acetic acid? *J. Phys. Chem. A*. 117,10997-11005(2013).
- 313 15. Zhang, F. et al. Theoretical study on desulfurization mechanisms of a coal-based
314 model compound 2-methylthiophene during pyrolysis under inert and oxidative
315 atmospheres. *Fuel*. 257,1-9(2019).
- 316 16. Li, T. et al. DFT research on benzothiophene pyrolysis reaction mechanism. *J.*
317 *Phys. Chem. A*. 123:796-810(2019).
- 318 17. He, F. et al. Quantum chemistry calculations on the mechanism of isoquinoline
319 ring-opening and denitrogenation in supercritical water. *Ind. Eng. Chem. Res.*
320 56,1782-1790(2017).
- 321 18. Hazra, M. K. Sinha A. Formic acid catalyzed hydrolysis of SO₃ in the gas phase:
322 a barrierless mechanism for sulfuric acid production of potential atmospheric

- 323 importance. *J. Am. Chem. Soc.* 133,17444-17453(2011).
- 324 19. Zhang, Y. et al. Decomposition of formic acid in supercritical water. *Energy*
325 *Fuels.* 24,95-99(2010).
- 326 20. Gao, Z. et al. Micro-mechanism of water molecule adsorption on lignite surfaces.
327 *Journal of Chinese Society of Power Engineering* 36,258-264(2016). (in Chinese)
- 328 21. Wang, G. et al. Mechanism of water polymer adsorption on lignite molecule.
329 *Coal Engineering.* 50,136-140(2018). (in Chinese)
- 330 22. Nie, B. et al. Micro-mechanism of coal adsorbing water. *Journal of China*
331 *University of Mining & Technology.* 33,379-383(2004). (in Chinese)
- 332 23. Gao Z. et al. DFT study of water adsorption on lignite molecule surface. *J. Mol.*
333 *Model.* 27:1-19(2017).
- 334 24. Frisch, M. J. et al. *Gaussian 09, Revision E.01.* Wallingford, CT: Gaussian Inc;
335 2013.
- 336 25. Zhao, Y. Truhlar DG. The M06 suite of density functionals for main group
337 thermochemistry, thermochemical kinetics, noncovalent interactions, excited
338 states, and transition elements: two new functionals and systematic testing of four
339 M06-class functionals and 12 other functionals. *Theor. Chem. Account.*
340 120,215-241(2008).
- 341 26. Zhao, Y., Truhlar D.G. Density functionals with broad applicability in chemistry.
342 *Acc. Chem. Res.* 41,157-167(2008).
- 343 27. Grimme, S. et al. Effect of the damping function in dispersion corrected density
344 functional theory. *J Comput. Chem.* 32,1456-1465(2011).

- 345 28. Burns, L. A. et al. Density-functional approaches to noncovalent interactions: A
346 comparison of dispersion corrections (DFT-D), exchange-hole dipole moment
347 (XDM) theory, and specialized functionals. *J. Chem. Phys.*
348 134,084107-084125(2011).
- 349 29. Vasiliou, A. K. et al. Modeling oil shale pyrolysis: high-temperature
350 unimolecular decomposition pathways for thiophene. *J. Phys. Chem. A.*
351 121,7655-7666(2017).
- 352 30. Huang, X. et al. A Density Functional Theory study on pyrolysis mechanism of
353 lignin in hydrogen plasma. *Ind. Eng. Chem. Res* 52,14107-14115(2013).
- 354 31. Johnson E. R. et al. Revealing noncovalent interactions. *J Am Chem Soc*
355 132,6498-6506(2010).
- 356 32. Lu, T., Chen F. Multiwfn: A multifunctional wavefunction analyzer. *J. Comput.*
357 *Chem.* 33,580-592(2012).
- 358 33. Humphrey, W. et al. VMD: Visual molecular dynamics. *J. Mol. Graphics.*
359 14,33-38(1996).
- 360 34. Canneaux, S., Bohr, F., Henon, E. Kisthelp: a program to predict thermodynamic
361 properties and rate constants from quantum chemistry results. *J. Comput. Chem.*
362 35,82–93(2014).
- 363 36. Vernon, L. W. Free radical chemistry of coal liquefaction: role of molecular
364 hydrogen. *Fuel.* 59:102-106(1980).
- 365 37. Zhai, Y. H. et al. Effects of water vapor and temperature on NO_x and CO
366 emissions during converter gas combustion. *Fuel.* 256,1-6(2019).

- 367 38. Kozłowski, M. XPS study of reductively and non-reductively modified coals. Fuel.
368 83,259-265(2004).
- 369 39. Gerald, J. et al. Hydrogen Sulfide Formation Over Automotive Oxidation
370 Catalysts. JSTOR. 84,750002-223, pp.477-484(1975).
- 371 40. Luo, Q. et al. Experimental Study of Gaseous Sulfur Species Formation during
372 the Steam Hydrogasification of Coal. Energy Fuels. 28,3399-3402(2014).
- 373 41. Eyring, H. et al. Basic chemical kinetics [M], Wiley, (1980).

Figures

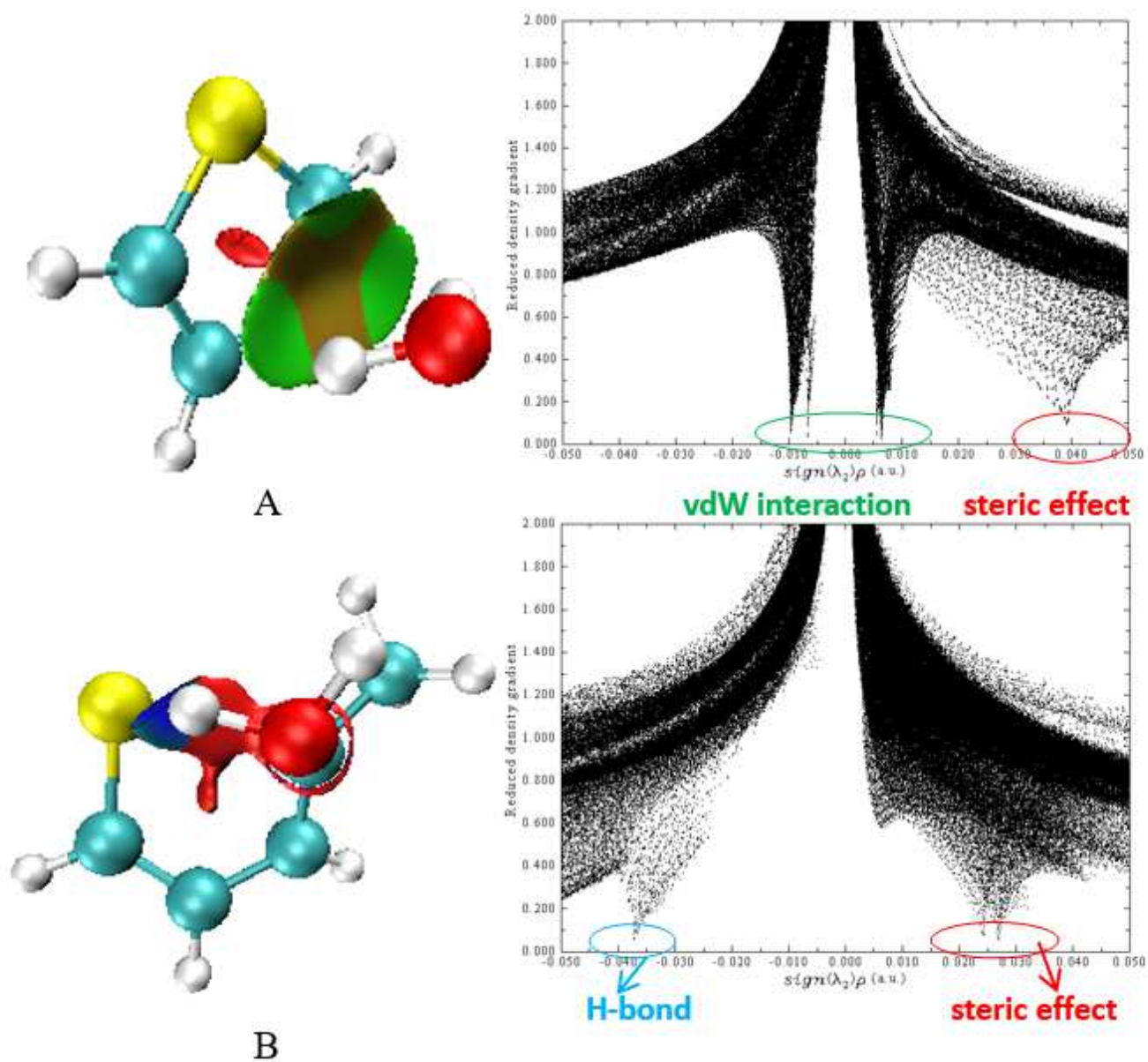


Figure 1

The RDG diagrams of complexes (i.e., complex A and B) formed by two typical thiophene sulfurs with H₂O (complex A is about the complex of thiophene and mono-H₂O; complex B is about the complex of mono-H₂O and 2-methyl thiophene.)

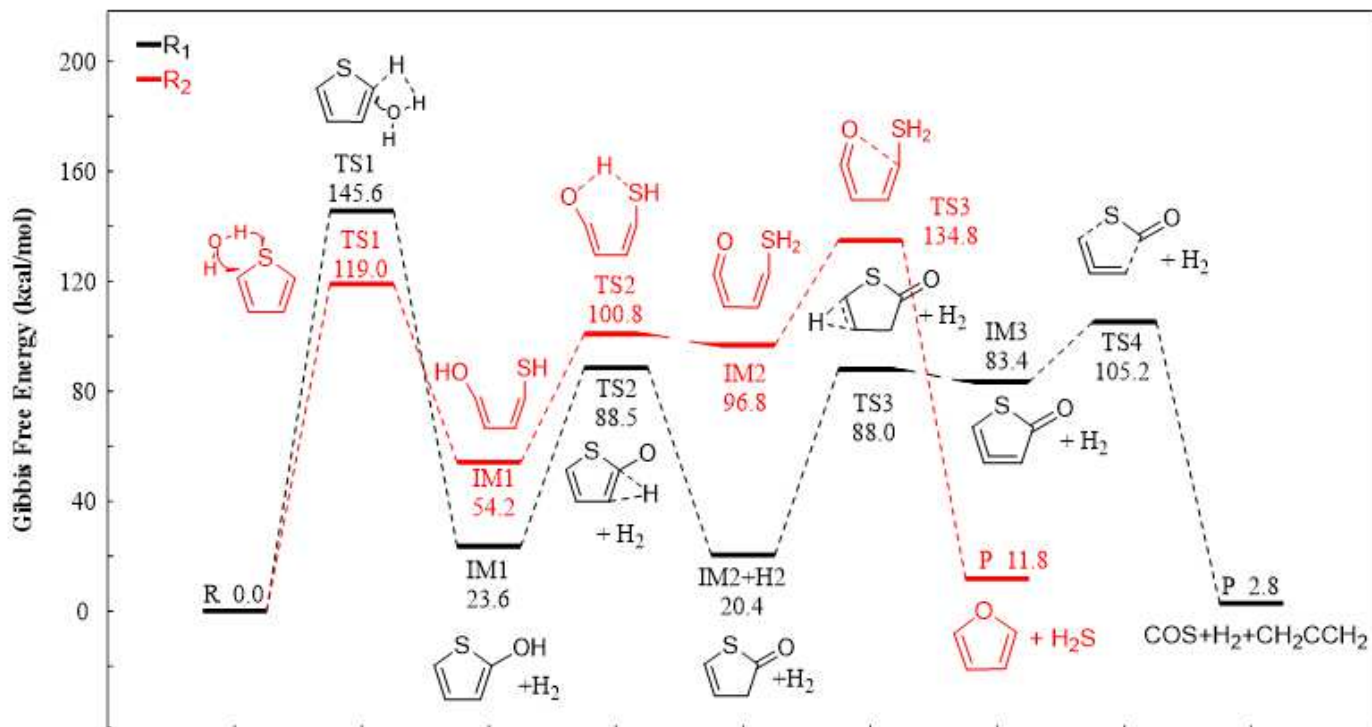


Figure 2

The energy diagram of thiophene and mono-H₂O forming COS (R₁) and H₂S (R₂) at 1200K

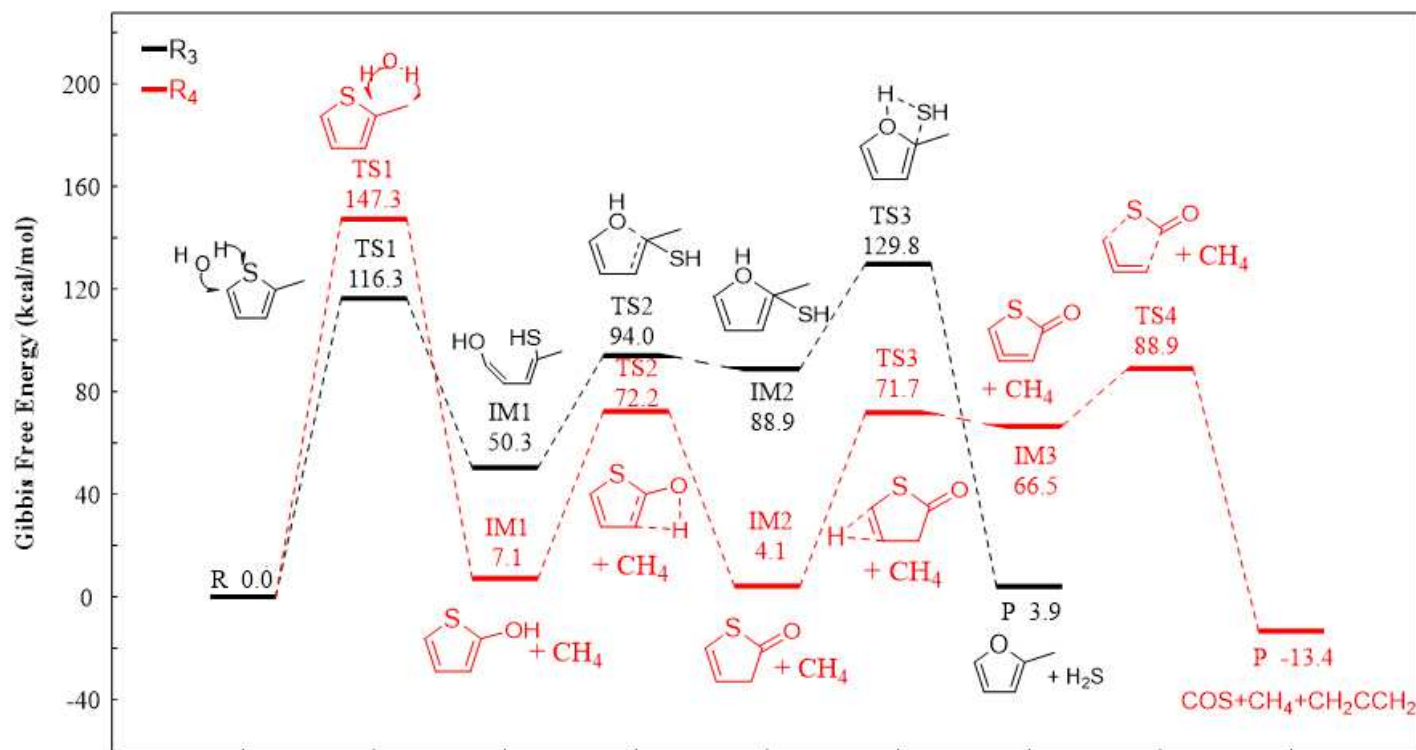


Figure 3

The energy diagram of 2-methyl thiophene and mono-H₂O forming H₂S (R3) and COS (R4) at 1200K.

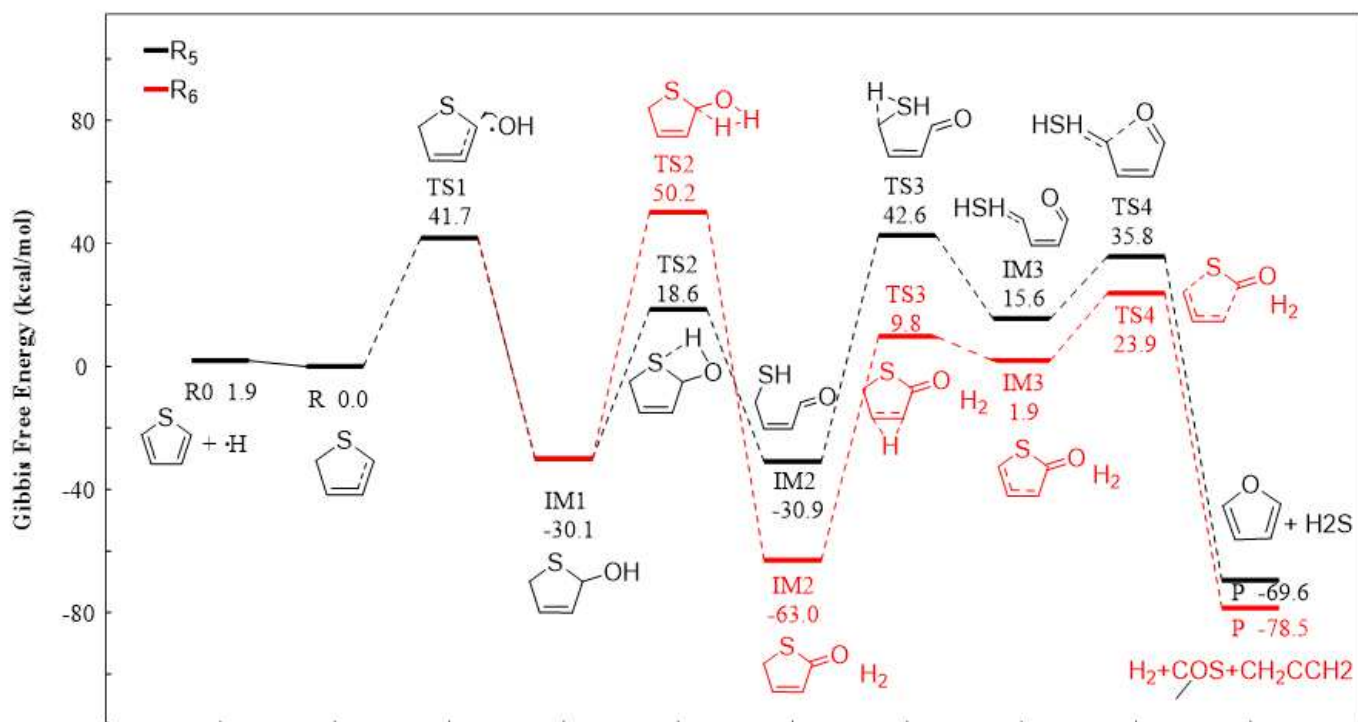


Figure 4

The energy diagram of thiophene and free radicals forming H₂S (R5) and COS (R6) at 1200 K

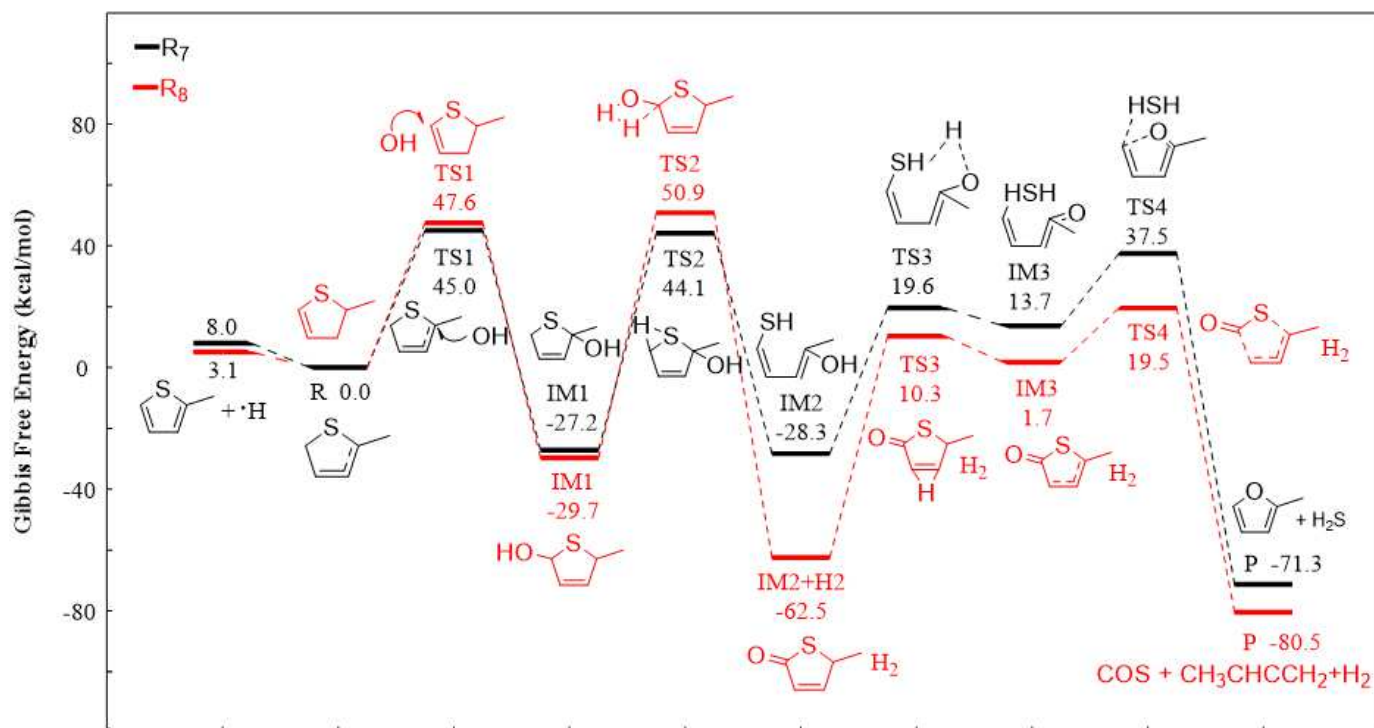


Figure 5

The energy diagram of 2-methyl thiophene and free radicals forming H₂S (R7) and COS (R8) at 1200 K